# Targeted Reinforcement of Macrophage Reprogramming Toward M2 Polarization by IL-4-Loaded Hyaluronic Acid Particles

Mohammad-Ali Shahbazi,*,[†,§] Mahsa Sedighi,[⊥] Tomás Bauleth-Ramos,[†,#,∇,○] Krishna Kant,[◆] Alexandra Correia,[†] Narges Poursina,[∥] Bruno Sarmento,[#,∇,○] Jouni Hirvonen,[†] and Hélder A. Santos*,[†,‡]

[†]Drug Research Program, Division of Pharmaceutical Chemistry and Technology, Faculty of Pharmacy and [‡]Helsinki Institute of Life Science (HiLIFE), University of Helsinki,Helsinki FI-00014, Finland

[§]Department of Pharmaceutical Nanotechnology, School of Pharmacy and [∥]Department of Pharmaceutical Biomaterials, School of Pharmacy, Zanjan University of Medical Sciences, Zanjan 56184-45139, Iran

[⊥]Division of Nanobiotechnology, Department of Life Sciences Engineering, Faculty of New Sciences and Technologies, University of Tehran, Tehran 14399-57131, Iran

[#]Instituto de Investigação e Inovação em Saúde (I3S) and [∇]Instituto de Engenharia Biomédica (INEB), University of Porto, Rua Alfredo Allen, 208, Porto 4200-135, Portugal

[○]Instituto Ciências Biomédicas Abel Salazar (ICBAS), University of Porto, Rua Jorge Viterbo 228, Porto 4150-180, Portugal

[◆]Department of Micro- and Nanotechnology, Technical University of Denmark, Ørsteds Plads, Kgs Lyngby DK-2800, Denmark

**ABSTRACT:** Alteration of macrophage polarization from inflammatory (M1) to anti-inflammatory (M2) phenotype can have striking implications for the regeneration of injured tissues, treatment of inflammatory diseases, and relief of autoimmune disorders. Although certain cytokines like interleukin (IL)-4 and IL-13 are capable of inducing M2 macrophage polarization, their therapeutic potential in vivo is suffering from low efficacy due to their instability and poor access to target cells. Here, we report the synthesis of IL-4-loaded hyaluronic acid (HA) particle for the targeted delivery of cytokines through the high affinity of HA to CD44 receptors of macrophages. HA carriers composed of low, middle, and high molecular weight (MW) polymers were synthesized using divinyl sulfone (DVS) cross-linking. The MW of HA had a negligible effect on the physicochemical properties and biocompatibility of the macrophages, but as an indicative of M2 polarization, a significant change in the arginase-1 (Arg-1) activity, TNF-$\alpha$ release, and IL-10 secretion was observed for the HA particles prepared with high MW polymers. Therefore, these particles were loaded with IL-4 for simultaneous macrophage targeting and M1 to M2 reprogramming, evidenced by a remarkable increase in the Arg-1 to iNOS ratio, as well as CD163 and CD206 upregulation in the M1 macrophages, which were initially triggered by lipopolysaccharide and interferon-$\gamma$.

IL-4 loaded HA particles — Cytokine targeting to M1 macrophages — M2 macrophage polarization
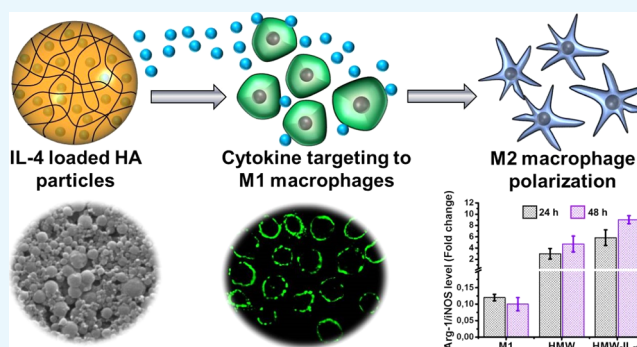
## 1. INTRODUCTION

Autoimmune disorders (ADs) are categorized as chronic diseases derived from an imbalance between stimulatory and regulatory mechanisms of the immune system, strongly affected by the genetic predisposition and environmental condition.[1−4] The trigger of immune pathways and systemic inflammatory responses in AD may result in the damage of healthy tissues by over-reacted immune cells. Many of the proposed immunoregulatory approaches against ADs are developed based on the blockage of the interaction between antigen-presenting cells and T cells.[5−8] Owing to the antigenic complexity of ADs and the need to simultaneously target multiple autoreactive T-cell specificities, traditional antigen-specific approaches have been shifting toward new investigation for more advanced and effective therapy of ADs

through the restoration of homeostasis in the immune function and tissue repair by macrophage reprogramming into immunoregulatory phenotypes.[9−11]

Macrophages are present in almost all the organs of adult mammals and contribute significantly to balanced immunity and tissue homeostasis, recognized as a key capability to treat autoimmune diseases through their polarization switching from activated inflammatory M1 phenotype to M2 tissue regenerating macrophages. The polarization of macrophages can be stimulated by different noninflammatory biomolecules, such as interleukin (IL)-4, IL-10, and IL-13.[12−15] M1 macrophages are
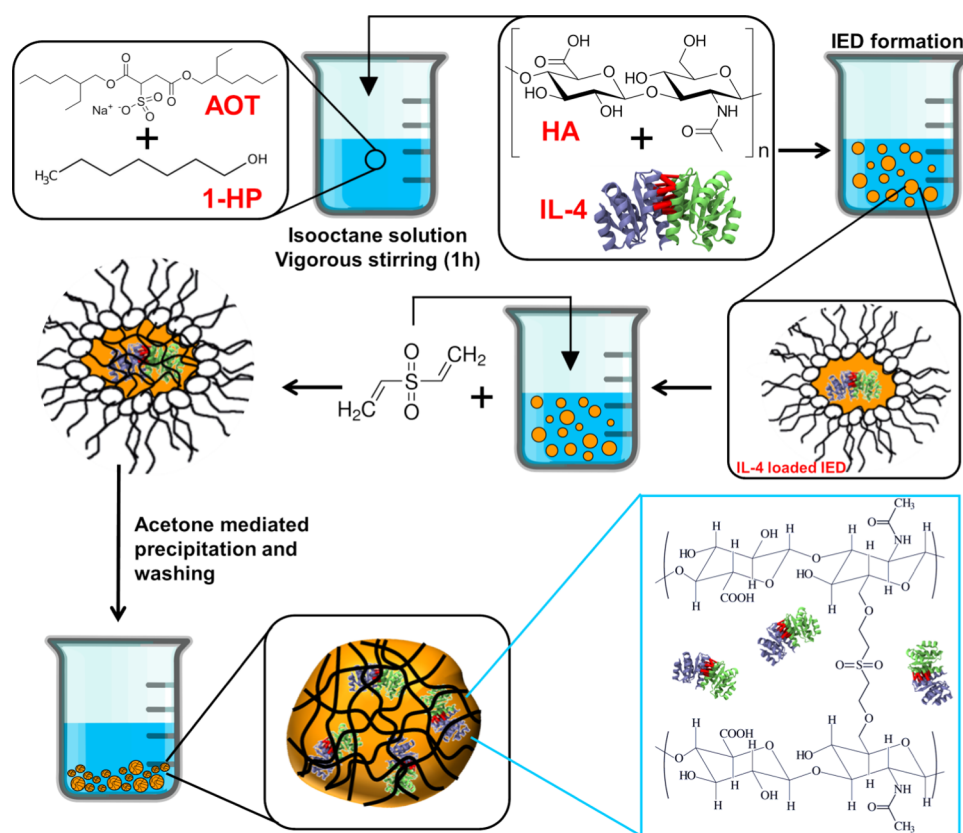
**Figure 1.** Schematic illustration of the synthesis procedure for HA particles containing IL-4 within the dioctyl sulfosuccinate sodium salt (AOT) reverse micelles. HA polymer solution containing IL-4 was added into the isooctane containing AOT and 1-heptanol (1-HP), forming inverse emulsion droplets through the coverage of the HA and IL-4 within the amphiphilic AOT chains. Next, DVS addition resulted in the covalent binding of HA chains and the formation of interpenetrating networks, which are able to retain the IL-4 intact for further targeting to macrophages through the high tendency of HA toward CD44 surface ligands.

mostly overexpressed in ADs, and their suppression through these cytokines can reduce the inflammatory reactions within the body. For example, there has been intensive research on the therapeutic effects of IL-4 on various inflammatory disease models. Nevertheless, there are big challenges associated with the rapid degradation and diminished bioactivity of unprotected IL-4 in the blood circulation, as well as poor targeting to the cells of interest.[16,17] Therefore, an efficient delivery system is required to protect and specifically target anti-inflammatory cytokines (e.g., IL-4) to the effector cells with the aim of blocking pathogenic inflammation without impairing immunity against infections and tumors, resulting in the expansion of their clinical applications.

Kim et al. suggested that extralarge pores mesoporous silica nanoparticles (XL-MSNs) possess high clinical potential for modulating immune systems through high loading and delivery of IL-4 as an M2-polarizing cytokine in vitro and in vivo. IL-4-loaded XL-MSNs significantly induced polarization of M2 macrophage in comparison to soluble IL-4.[10,18] However, it is presumable that by specific targeting of the IL-4 to the macrophages, better M2 polarization responses can be observed. For this purpose, CD44 targeting polymers, such as hyaluronic acid (HA), can be applied since the macrophages are recognized for the high expression of this protein on their surface.[19−22]

HA is an anionic biologically active linear polymer with a variety of molecular weights (MWs). It is biocompatible, can be found in the extracellular matrix, and is responsible for important biological functions, including cell interactions and movements, cell proliferation, cell differentiation, etc.[23,24] HA has emerged as an ideal and versatile drug delivery vehicle due to its water solubility, biodegradability, nontoxic nature, facile chemical functionalization, and capability to be used as carriers for different payloads.[25−27] Confirmed by previous studies,[28] the MW-dependent effect of HA on macrophage polarization is attributed to the induction of different stimulatory or suppressive signaling pathways after HA interaction with macrophages through surface receptors, such as CD44, hyaluronan-mediated motility receptor, Toll-like receptor 2 (TLR2), Toll-like receptor 4 (TLR4), and scavenger receptor Stabilin-2 (STAB2).[19,29] These receptors, particularly CD44, have been introduced as the best candidate for HA-mediated targeting of various cell types, including macrophages, by which the circulation time of small particles can be extended and the polarization process can be induced.[30,31] As an example, plasmid-DNA-encapsulated HA-poly(ethyleneimine) nanoparticles were designed with the average size of 186 nm to modulate macrophage reprogramming.[32]

As far as we know, there is no report demonstrating the capability of pure HA particles to encapsulate immunoregulatory cytokines for macrophage reprogramming. Therefore, we contemplated the design of such carriers to concurrently protect and deliver IL-4 biomolecules to the macrophages. The suggested platform can be used for combined targeting and polarization of macrophages toward M2 phenotype. The developed IL-4-loaded carrier is composed of HA polymer
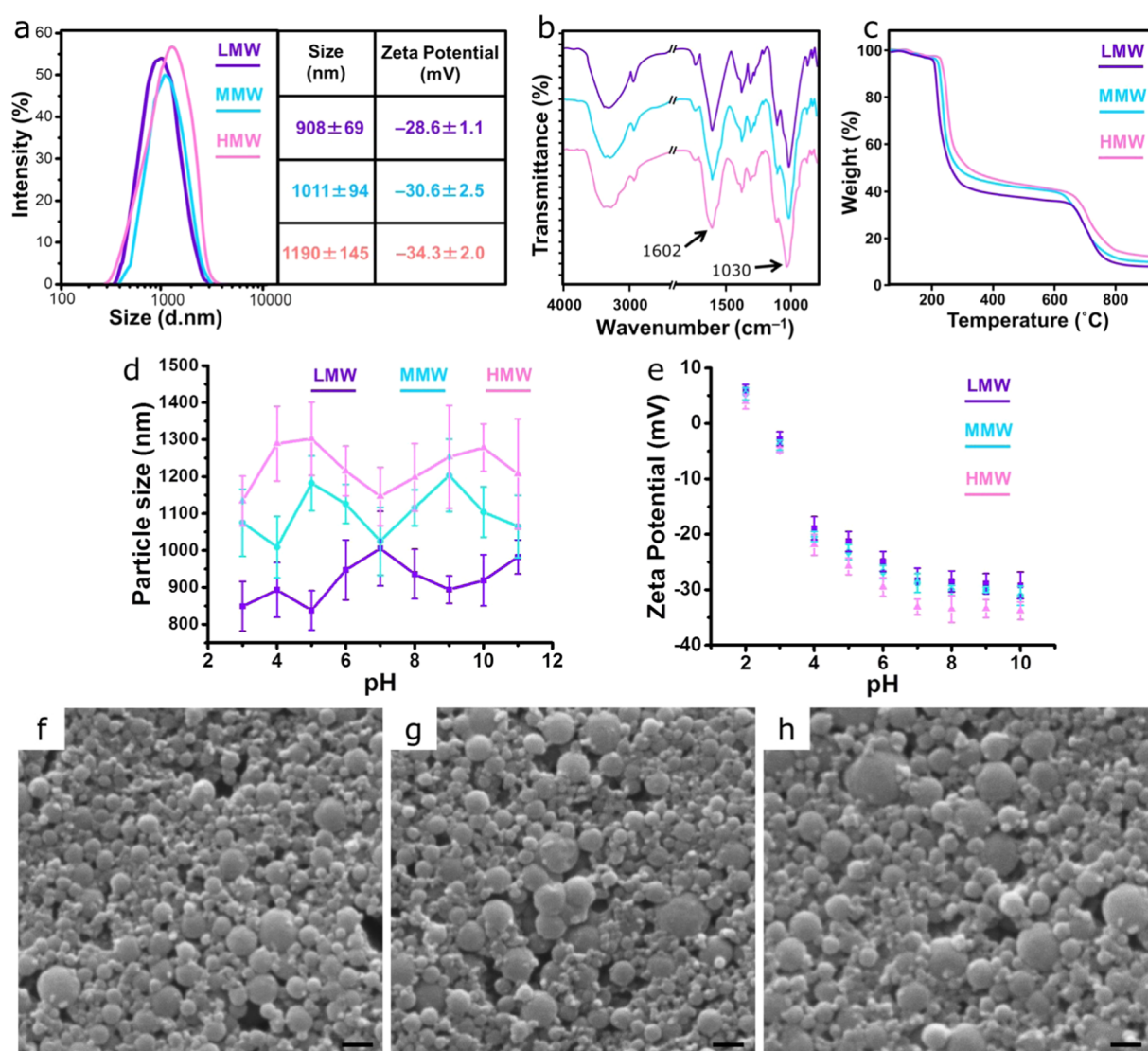
**Figure 2.** Physicochemical characterization of the HA particles prepared by HA polymers with different MWs. LMW, MMW, and HMW represent the particles prepared with low, middle, and high MW HA, respectively. (a) Size and $\zeta$-potential of the HA particles. (b) Fourier transform infrared (FTIR) spectra of HA particles, indicating bands at 1602 cm$^{-1}$ for −COOH groups of the HA and at 1030 cm$^{-1}$ for S−O and C−S stretching frequencies of DVS. (c) Thermogravimetric analysis (TGA) of the HA particles. (d) Size−pH correlation of the HA particles. (e) $\zeta$-Potential of the particles at different pH conditions in a 0.01 M KCl solution. The pH was adjusted using 0.1 M NaOH and 0.1 M HCl. (f−h) Scanning electron microscopy (SEM) images of the HA particles prepared by low (f), middle (g), and high (h) MW of the HA polymer. Scale bars are 2 $\mu$m.

assembled through the formation of water-in-oil inverse microemulsion droplet and divinyl sulfone (DVS)-mediated covalent cross-linking. The process of carrier synthesis is schematically summarized in Figure 1. The physicochemical characterization, biocompatibility, and cellular effect of HA particles made of low, medium, and high MW of the polymer were assessed. The one with the highest M2 polarization capability was then chosen for the loading of IL-4 and immunity modulation via targeted delivery of the IL-4 cytokine to obtain synergistic M2-polarizing effect of the HA polymer and the drug on the macrophages.

## 2. RESULTS AND DISCUSSION

**2.1. Physicochemical Characterization of HA Particles.** HA is a very important natural polymer, existing in different cells and tissues of the human body with key biological functions in cell signaling and proliferation, organization of the extracellular matrix, joint lubrication, and

wound healing.[20,24,33−35] Owing to its biocompatibility and biodegradation, great attention toward drug delivery, biotargeting, and tissue-engineering features of this polymer has been given in recent years.[24,25,30,31,33,36,37] Since the MW-dependent biological impacts of HA polymer have been previously proved,[28] in the current study, we aimed to figure out the effect of HA particles, prepared with varied MWs of the polymer, on the macrophages and then select the best one for further investigation of IL-4 loading and synergistic M2 polarization.

Spherical-shaped particles were produced by means of various MWs of HA within the reverse micelles of AOT. Figure 2a demonstrates that the average size of the particles instantly increased from ∼900 nm to 1.2 $\mu$m as a function of MW increment (LMW, MMW, and HMW are representative of the HA particles prepared by low, middle, and high MW polymers, respectively). This observation can be associated with the longer polymer chains of the polymer with higher
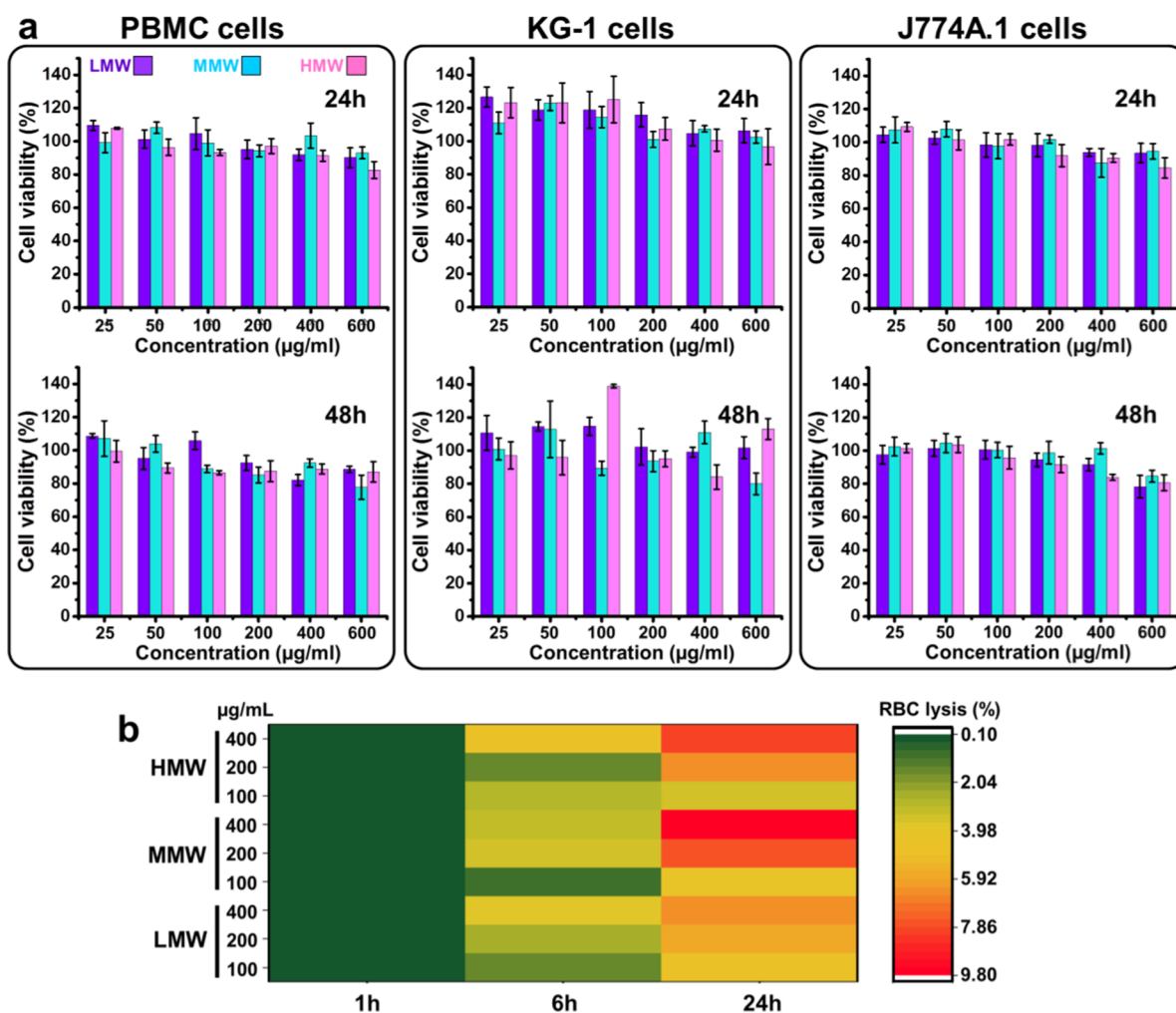
**Figure 3.** (a) Biocompatibility of the particles prepared with low, middle, and high MWs of the HA polymer. The effect of HA's MW on cell viabilities of PBMC, KG-1, and J774A.1 cells after treatment with the particles at 37 °C for 24 and 48 h. The experiments were performed for different HA concentrations in a range of 25−600 μg/mL. (b) Hemocompatibility of the HA-based particles during the screening period of 24 h. The tested concentrations include 100, 200, and 400 μg/mL of HA particles. LMW, MMW, and HMW are representative of the HA particles prepared by low, middle, and high molecular weight polymers, respectively.

MW, which produced bigger DVS-mediated chemically cross-linked networks.

The surface charges of all types of particles were also measured. The negative surface of the particles prepared with HMW polymer was significantly higher than the particles prepared with LMW polymer (Figure 2a). It is plausible that the higher number of carboxyl groups on HA polymer with a longer chain resulted in a clear shifting of the $\zeta$-potential of the prepared particles toward lower negative values.

Next, attenuated total reflectance-Fourier transform infrared (ATR-FTIR) spectra of HA particles were taken to demonstrate successful formation of the particles through the cross-linking of the HA and DVS. In all types of the prepared particles, distinctive bands at 1602 cm$^{-1}$ were observable for −COOH functional groups of the disaccharide units in HA, and the bands at 1030 cm$^{-1}$ appeared for S−O and C−S stretching frequencies of DVS (Figure 2b).

Thermal behavior of the HA particles showed no remarkable effect of the MW on the TG thermograms that were taken by 10 °C/min heating rate (Figure 2c). In general, two distinct degradation temperatures were observed for HA particles. The first step of degradation started at 210−230 °C depending on

the MW of the polymer. In this step, 50−60% of the total weight was lost before reaching 300 °C. When the temperature reached 650 °C, the second degradation pattern started and continued up to 850 °C in which the remained weights of all types of the particles were less than 15%.

To investigate the stability of the HA particles in different pH values (ranging from 3 to 11), the changes in particle size and $\zeta$-potential of HA particles were measured with dynamic light scattering (DLS) and their corresponding graphs are shown in Figure 2d. The HA particles did not show any significant change in their size with pH alteration from 3 to 11. Despite the presence of carboxyl groups, the particles did not swell in basic pH conditions due to their compact and nonporous nature achieved by high chemical cross-linking with DVS. In contrast, the surface $\zeta$-potential of all HA particles changed from ca. +5 to −30 mV by increasing the pH from 2 to 10 (Figure 2e). The positive surface charge of the HA particles at pH 2 is related to the high rate of protonation on hydroxyl groups of the particles.

The SEM images of the HA particles (Figure 2f−h) showed spherical morphology, which demonstrates no impact of the polymer MW on the shape of the final product. In addition, the
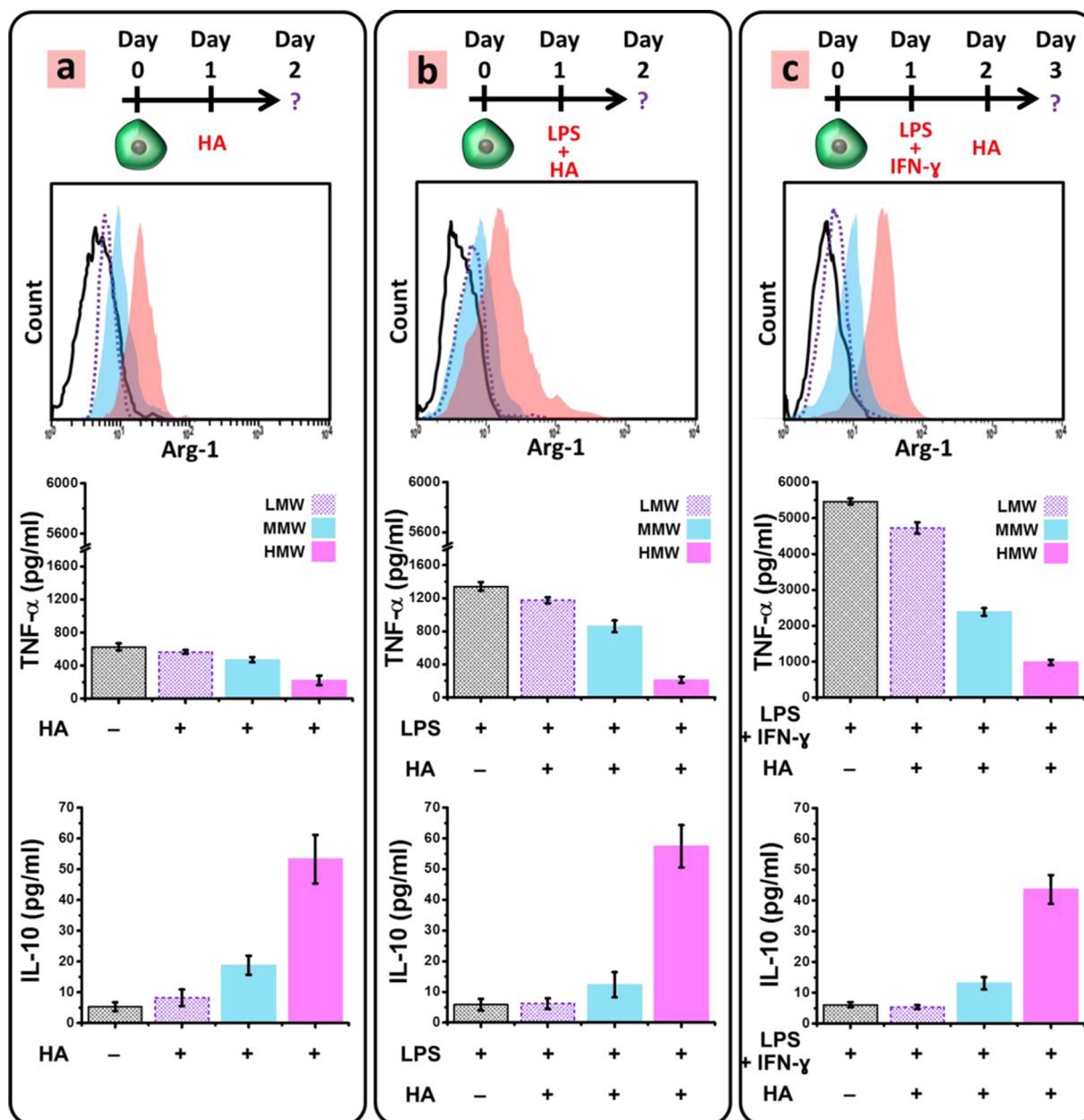
**Figure 4.** Impact of MW of the HA particles on Arg-1 expression, TNF-$\alpha$ suppression, and the induction of IL-10 secretion in the (a) resting, (b) LPS-triggered, and (c) classically activated J774A.1 macrophages. The schematics demonstrate the time course of the experiments. LMW and MMW HA particles had minimal eliciting effect on M2 polarization since very slight changes in the expressions of Arg-1 and IL-10 release were observed. In contrast, HMW HA particles could more remarkably reduce the level of TNF-$\alpha$ in all three tested conditions and could also increase the Arg-1 and IL-10 levels. Error bars represent mean ± standard deviation (SD) of three independent experiments.

observation is in line with the data achieved from DLS measurement, showing the majority of the particles with the size of around 1 $\mu$m. However, bigger particles could also be observed in all samples, varying in the range of 1−5 $\mu$m.

**2.2. In Vitro Biocompatibility.** To assess the in vitro safety and high cytocompatibility of different HA particles fabricated by various MWs of the polymer, a cell viability assay was performed on different cell lines, including peripheral blood mononuclear cells (PBMC), KG-1 macrophages, and J774A.1 macrophages after treatment with the carriers at a concentration range of 25−600 $\mu$g/mL for 24 and 48 h at 37 °C. As shown in Figure 3a, all tested concentrations showed high cytocompatibility on all three cell lines tested. The viability of the cells slightly reduced by increasing the

incubation time and the concentration of the particles. However, all values remained desirably above 80% in all time points of various concentrations. Previous studies have shown the distinct effect of the MW on cellular function of the cells treated with HA.[28,38] HMW HA was able to suppress cell cycle via binding to CD44, whereas cell proliferation was stimulated by LMW HA when interacted with CD44.[22,37,39,40] However, in our study, we just observed 20% variation in the viability of the cells exposed to particles prepared with different MWs of HA polymer (Figure 3a). In another study, researchers have shown the promotion of cell proliferation after treatment with HMW HA.[21] These differences and controversies might be attributed to the cell type, variation of the polymer MW in different studies, and the form of HA (e.g., polymer solution,

nanoparticles, microparticles, or as a coating layer for other nanomaterials) used for the studies. All these factors can affect the regulation of signaling pathways through the change in the internalization of the polymer into the cells.[25] Overall, these results showed acceptable in vitro safety and biocompatibility of HA-based particles, which can be therefore used as carriers for drug delivery applications.

**2.3. Hemocompatibility.** Red blood cells (RBCs) are the most abundant cells in the bloodstream and in very close contact with the particulate drug delivery systems after intravenous injection. Therefore, there is a risk of deformation and cell membrane damage if the particles are toxic.[41,42] To investigate the effect of the HA's MW on the lysis of RBCs, HA-based particles, in a concentration range of 100−400 μg/mL, were exposed to the hemoglobins. When treated for 1 and 6 h, the RBC lysis was much less than the longer exposure time (24 h) in all the HA-based particles tested (Figure 3b), demonstrating the dependency of the hemolysis rate to the exposure time. Whereas 100 μg/mL of all the HA-based carriers induced less than 4% hemolysis after 24 h, 400 μg/mL of the particles could meaningfully enhance the rate of hemolysis to more than 9%, especially in cells treated by MMW HA-based particles. This indicates concentration and MW dependency in hemolysis effect of HA particles.

Overall, our data represented a direct relationship of concentration, MW, and exposure time with the hemolysis rate of the RBCs. The induction of hemolysis was higher for MMW and HMW HA-based particles as compared to the LMW HA-based counterparts; however, it was less than 10% in all cases. The high hemocompatibility of the HA particles can be explained through the hydrophilicity and negative surface charge of the particles that prevent their interaction and penetration into the RBCs due to surface negative charges and hydrophobic lipid bilayer of the plasma membrane. The comparison of MWs showed that LMW HA-based particles caused lower hemolysis rate presumably due to the relatively weaker interaction with the cell surface. It can be due to varying structural conformations of HAs with various MWs in solution, resulting from differences in flexibility and viscosity of HA chains.[27]

**2.4. Impact of HA Particles on Resting and Activated Macrophages.** Depending on their cellular phenotype and cytokine secretion pattern, macrophages are able to either mediate or suppress inflammatory responses. Programmed switching of macrophages from an inflammatory (M1) to anti-inflammatory (M2) phenotype renders substantial benefit for the treatment of inflammatory and autoimmune diseases, as well as the regeneration of injured tissues. It was previously shown that the MWs of polymers have the capability of eliciting different biological responses.[20,25] In this regard, before IL-4 loading into the HA particles, the role of MW on the reprogramming of macrophages was investigated. To provide a synergistic effect for IL-4 payloads, we were looking for a polymer with M2-polarizing effect as a carrier for this cytokine. Therefore, the impact of particles prepared by low, middle, and high MWs of the HA polymer was investigated on the arginase-1 (Arg-1) expression, TNF-α release, and IL-10 production in resting macrophages, lipopolysaccharide (LPS)-stimulated macrophages, and LPS + IFN-γ costimulated macrophages (Figure 4).

For the resting macrophages shown in Figure 4a, Arg-1 expression was significantly upregulated after treatment with particles made of HMW HA, whereas treatment with LMW and MMW HA particles demonstrated lower population of the Arg-1 positive cells. Arg-1 expression on cell surface is a signature of M2 macrophage polarization.[10,43] TNF-α production in macrophages treated by HMW HA particles was also lower than other types of particles and the nontreated cells. Although this test was performed with the HA particles, the finding was in line with previous reports that showed the ability of the HMW HA polymer in solution form for the suppression of TNF-α production, known as an indicator of anti-inflammatory response for the M2 polarization of the macrophages.[28] This finding shows the potential of the developed particles with HMW HA polymer to develop drug-loaded carriers for AD therapy through M2 macrophage activity.

Next, the secretion of IL-10 was examined, and it demonstrated a significant upregulation in resting macrophages treated with HMW polymer compared to the other conditions examined. IL-10 is an anti-inflammatory cytokine generally produced by M2 macrophages, and the upregulation of IL-10 proves the successful transition from M1 to M2 phenotype via HA treatment. As expected, particles prepared by HMA HA could downregulate the production of M1 cytokines, such as TNF-α, but upregulate IL-10 secretion as a known M2 cytokine.[27] This finding suggests that not only the polymeric solution of HA, but also the particulate form of HMA HA can elicit M2 state from resting macrophages.

In the next step, HA and LPS were simultaneously exposed to the resting macrophages to mimic an acute classical inflammatory response against LPS, an antigen derived from Gram-negative bacterial wall. According to previous reports, LPS is able to mediate acute inflammation as a potent macrophage activator and to produce many inflammatory mediators, such as TNF-α and IL-6.[36,44] It is revealed in Figure 4b that the highest Arg-1 expression was acquired in macrophages treated with HMW HA particles, and other types showed no significant differences compared to the control. It is also shown that TNF-α secretion tended to increase in the presence of LPS that exemplifies the high sensitivity of macrophages to the inflammatory challenge with LPS. Cotreatment with LPS and HA particles resulted in contrary effect with decreasing TNF-α level in an MW-dependent manner. As it is clear in Figure 4b, macrophages treated with HMW HA particles decreased TNF-α secretion in a magnitude of six compared to the LPS-treated macrophages. In the case of IL-10, the highest secretion level was observed following treatment with HMW HA particles by which the activation of macrophages toward M2 phenotype is strongly feasible, whereas LPS alone and particles prepared by low and middle MW of HA did not have any capability to increase the secretion level of IL-10.

Next, the impacts of HA particles on classically activated macrophages were investigated in the presence of both IFN-γ and LPS. There are many chronic diseases associated with classically activated state of macrophages as it can have huge detrimental effects on various tissues.[45−48] Therefore, we tried to mimic the classically activated macrophages through pretreatment with both IFN-γ and LPS to represent a robust inflammatory response before exposure to HA particles. Development of a particulate system, which can alter the population of such macrophages, would have a remarkable role in the alteration of macrophage function within damaged tissue. As shown in Figure 4c, it is obviously clear that the greatest increase in Arg-1 expression was observed in
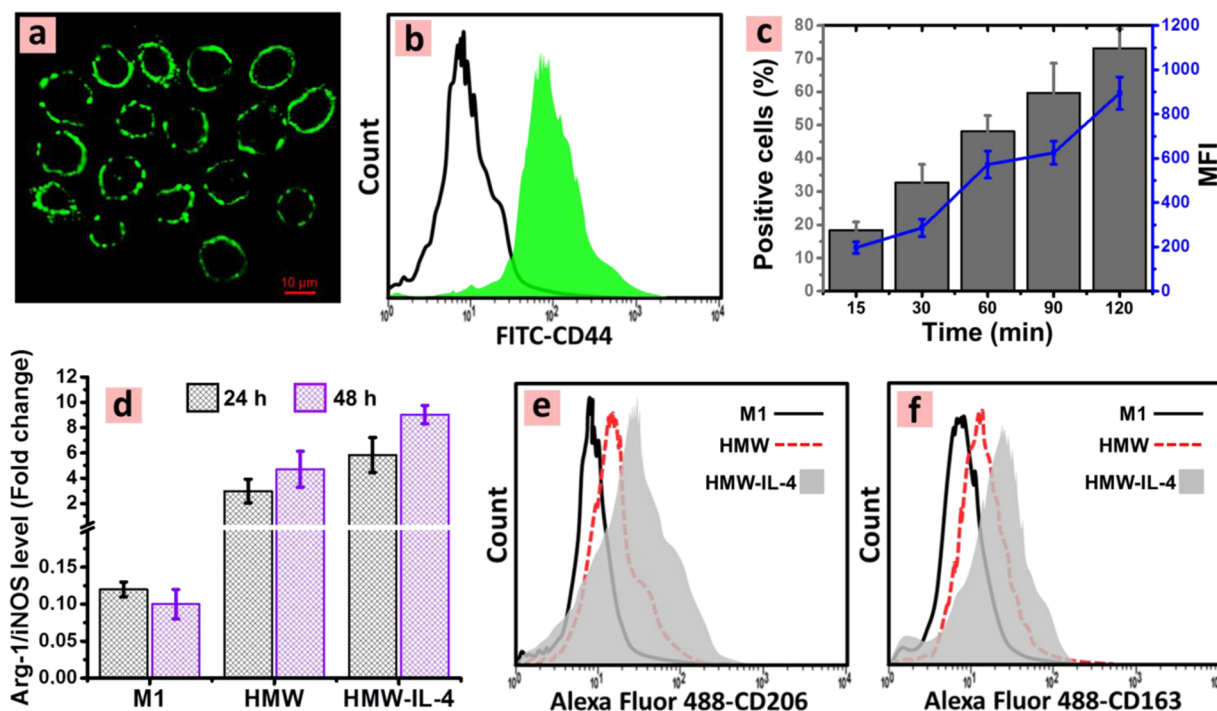
**Figure 5.** Analysis of CD44 expression in J774A.1 macrophages using (a) confocal microscopy and (b) flow cytometry. (c) Cellular uptake of the HMW particles of HA in J774A.1 macrophages. The uptake of the particles into the cells increased over time. (d) Change in the ratio of Arg-1 to iNOS after 24 and 48 h of treatment with IL-4-loaded (HMW-IL-4) and unloaded (HMA) HA particles. This is indicative of the M2/M1 ratio of the macrophages, which were initially triggered by LPS and IFN-$\gamma$ toward the M1 phenotype. (e, f) Flow cytometry histograms of the CD206 and CD163 expressions in LPS- and IFN-$\gamma$-stimulated J774A.1 macrophages without and with exposure to IL-4-loaded (HMW-IL-4) and unloaded (HMA) HA particles for 48 h at the concentration of 100 $\mu$g/mL (1.2 mL).

macrophages treated with HMW HA, which was significantly higher than those of LMW and MMW HA particles. Compared to LPS-treated macrophages, TNF-$\alpha$ production was increased fourfold more in the presence of LPS + INF-$\gamma$, demonstrating the potential of INF-$\gamma$ for macrophage activation in certain chronic inflammatory conditions.[36] In this experiment, macrophages were classically activated for 24 h, and then, the media were replaced with media containing HA particles. After 24 h of the treatment with HA particles with various MWs, increased Arg-1 expression and IL-10 secretion, as well as reduced level of TNF-$\alpha$ production was observed for HMW particles. In all cases, an MW-dependent trend was observed. In general, these data prove that treatment with HMW HA particles elicits signals needed for the M2 polarization of macrophages.

**2.5. Cellular Targeting and M1 to M2 Repolarization.** The main prerequisite for the targeting of macrophages by HA particles is the high availability of CD44 receptor on the surface of the cell membrane. Therefore, the expression of CD44 was evaluated on J774A.1 macrophages by confocal microscopy and flow cytometry instruments. Figure 5a,b shows the strong fluorescence of the cell membrane stained with FITC-CD44 antibody and a clear shift in the histogram of J774A.1, respectively. The indicated high expression of CD44 on the cell membrane confirms the potential of HA particles to target these cells. Time-dependent efficient in vitro cellular uptake (Figure 5c), which occurred by the HMW particles of HA, could possibly confirm CD44 receptor recognition by the particles and subsequent promotion in their interaction with the cell membrane and enhanced endocytosis.[49] In the polymeric backbone of the HA, the C6-OH of N-acetylglucos-amine (GlcNAC) forms hydrogen bonding to CD44 on the

macrophages. HA is a polymer with repetitive units of the GlcNAC and another ring functionalized with −COOH and −OH. Considering the low amount of the DVS and observed data of efficient CD44 targeting, it seems there are many of the free C6-OH of GlcNAC groups in the structure of HA for CD44 targeting after conjugation with DVS, confirmed by the FTIR bond at 3500 cm$^{-1}$, corresponding to −OH groups of the HA particles (Figure 2).

The internalization of the IL-4-loaded particles would then increase the expression and production of M2-polarizing genes, proteins, and biomolecules, as shown in Figure 5d−f, and the switching of M1 polarized macrophages toward M2 phenotype. In this experiment, J774A.1 macrophages were first treated with LPS and IFN-$\gamma$ for 16 h to increase the expression of M1 markers.[32] Next, the stimulated cells were treated with the IL-4-loaded HA particles, and the expressions of M2 markers were determined. The yield of the particle formation was ca. 90%, and the calculated amount of IL-4 in 100 $\mu$g of HA particles was 51.4 ± 2.8 ng (equal to a loading efficiency of ca. 92.5%).

The M1 macrophages present high expression levels of CD80, TNF-$\alpha$, and iNOS, whereas the M2a polarization of macrophages is associated with a decrease in M1 markers and an increase in Arg-1, CD163, and CD206 levels. Therefore, to investigate if IL-4-loaded HA particles could repolarize the macrophages from M1 to M2a phenotypes, Arg-1/iNOS (Arg-1/iNOS) ratio was measured by qPCR in the M1 phenotype cells treated with the particles for 24 and 48 h (Figure 5d). According to previous reports,[50] the M2 polarization of macrophages is associated with a decreased expression of iNOS and an increase in Arg-1 level. Therefore, the ratio of Arg-1 to iNOS can be an indication of macrophage polarization to M2 phenotype. As shown in Figure 5d, the

Arg-1/iNOS ratio was remarkably low in the M1 macrophages, indicating the high expression of iNOS and low expression of Arg-1. In contrast, this ratio was dramatically increased after treatment with both unloaded and IL-4-loaded particles for 24 and 48 h. The Arg-1/iNOS ratio was higher in the IL-4-loaded particles compared to the unloaded counterparts at both time points, demonstrating the effect of IL-4 on the enhanced M2 repolarization of the macrophages. Furthermore, the observed time-dependent increase in the Arg-1/iNOS ratio can presumably be attributed to the sustained release of IL-4 within the cells after internalization.

As specific surface markers for M2a macrophages,[51] the change in the expressions of CD206 and CD163 was evaluated in the J774A.1 macrophages. Figure 5e,f show the histograms of CD206 and CD163 expressions in M1 J774A.1 macrophages exposed to the unloaded and IL-4-loaded particles for 48 h. The LPS- and IFN-γ-treated M1 macrophages were considered as control. The shift to the higher fluorescence intensity values was observed for both CD206 and CD163 proteins after treatment with the unloaded and loaded particles, indicating the upregulation of M2 surface markers. The shifting of the histogram was higher for the IL-4-loaded HA particles compared to the unloaded one. This result suggests that the loading of IL-4 plays a significant role in the efficient M2 polarization of the cells after the cellular uptake of the particles.

In general, the developed HA carriers could induce immunoregulatory responses against autoimmunity and inflammatory reactions, possibly without impairing immunity against infections or tumors that will be explored in the next steps. Dynamic switching of M1 and M2 macrophages has a key impact on the restoration of normal function in all tissues after injury or infection.[52−54] For example, it has been shown that metabolic diseases such as type 2 diabetes can be exacerbated by M1 macrophages but ameliorated by M2 ones.[46,55] IL-4 is one of the main anti-inflammatory cytokines that can suppress the secretion of proinflammatory cytokines and induce M2 polarization for the therapy of various inflammatory disease models.[13,15,16,47] Nevertheless, IL-4-mediated therapy is hampered due to the short half-life of this biomolecule and rapid degradation, and its compensation requires a high dose of the cytokine and toleration of inevitable systemic side effects.[10] This drawback was recently circumvented by viral transduction of the IL-4 gene.[56] Since the delivery of exogenous genes to human needs to meet certain safety regulations and cannot specifically affect the macrophages, our present work aimed for the first time to demonstrate an efficient targeted delivery system for IL-4 toward CD44-positive macrophages for the future translation of exogenous IL-4 into clinic with minimal concern as compared to other suggested approaches.

## 3. CONCLUSIONS

In this study, the polarization of macrophages toward anti-inflammatory M2 phenotypes was reported by IL-4-encapsulated HA carriers. The HA particles were successfully synthesized from various MWs of the HA polymer using a simple method, and the characterization and toxicity studies showed their high safety and desirable properties for drug delivery. Further investigation demonstrated that HA particles prepared from HMW polymers significantly increase the anti-inflammatory markers of the macrophages, whereas the particles fabricated from LMW and MMW polymers had negligible effect on the induction of anti-inflammatory cytokines. Therefore, HMW polymer was used for IL-4 loading and M2 differentiation studies. The particles were able to efficiently interact by J774A.1 macrophages that express the CD44 receptor. Importantly, in vitro treatment of the M1 macrophages with IL-4-loaded HA particles enhanced the Arg-1/iNOS gene expression levels. Moreover, the CD206 and CD163 expressions were upregulated as the known markers of M2a macrophages. The results indicate that macrophages were successfully skewing their phenotype from M1 to M2 using the anti-inflammatory cytokine-loaded HA particle, suggesting its high potential for the targeted treatment of various auto-immune and inflammation-associated diseases.

## 4. EXPERIMENTAL METHODS

**4.1. Materials.** Dioctyl sulfosuccinate sodium salt (AOT), 2,2,4-trimethylpentane (isooctane, anhydrous), divinyl sulfone (DVS), 1-heptanol (1-HP), acetone dichlorofluorescin-diacetate, N-(3-dimethylaminopropyl)-N′-ethylcarbodiimide hydrochloride (EDC), N-hydroxysuccinimide (NHS), and lipopolysaccharide (LPS) were purchased from Sigma-Aldrich Chemical Co (Germany). CellTiter-Glo Luminescence Cell Viability assay kit was obtained from Promega Corporation. HA (sodium salt, 10−20, 151−300, and 1.01−1.8 kDa) was purchased from Lifcore Biomedical Co. Alexa Fluor 488 conjugated rabbit anti-CD163/M130 polyclonal antibody was purchased from Bioss Antibodies. Alexa Fluor 488-antimouse CD206 and CD44 antibodies were obtained from BioLegend. J774A.1-adherent murine macrophage cell line was obtained from the American Type Culture Collection. Fetal bovine serum (FBS) was from HyClone, Dulbecco's modified Eagle medium (DMEM) was from Cellgro, and penicillin/ streptomycin antibiotics were from Gibco Invitrogen. Specific primers of Arg-1 and iNOS2 were purchased from Eurofins MWG Operon. Recombinant Mouse IL-4 and enzyme-linked immunosorbent assay (ELISA) kits for IL-10, TNF-α, and IL-4 were obtained from R&D Systems.

**4.2. Synthesis of HA Microparticles.** HA microparticles were synthesized using the reverse micelle cross-linking technique and the formation of a water-in-oil inverse microemulsion droplets, as shown in Figure 1. The aqueous phase was prepared by dissolving HA in NaOH (0.2 M) at a concentration of 4 mg/mL. The organic phase was isooctane containing 0.2 M of AOT and 0.04 M of 1-HP in isooctane. To prepare the droplets, 0.25 mL of HA solution was added to 7.5 mL of isooctane containing 0.2 M of AOT and 0.04 M of 1-HP under vigorous agitation until a clear solution was obtained. Next, 4 μL of DVS cross-linker was added under vortexing, and the reaction was allowed to complete for 1 h under stirring at room temperature. Particles were precipitated using 100 mL of acetone and then collected by centrifugation at 10 000 rpm for 10 min. Next, the particles were washed three times with acetone and water mixture (1:1 v/v) and once with water before using them in other experiments.

**4.3. Characterization of the HA Particles.** The sizes (hydrodynamic diameter) and ζ-potentials of the HA particles prepared by low, middle, and high molecular weight HAs were measured using a Zetasizer Nano ZS instrument (Malvern Instruments Ltd, U.K.). For this purpose, particles were dispersed in 0.01 M of $KNO_3$ solution in water and then sonicated for 20 min to obtain highly dispersed particles.

The changes in the sizes of particles synthesized with LMW, MMW, and HMW HAs were determined in different pH

values, ranging from 2 to 11, using a particle size analyzer. The pH was adjusted with 1 M of HCl and 1 M of NaOH. The measurements were performed in a solution of NaCl (100 mM) to ensure fixed ionic strength for all measurements. In addition, the surface characterization of the particles was investigated by $\zeta$-potential measurements at various pH values in 0.01 M of KCl solution. Before the study, the HA particles were passed through paper filters with pore size >2 $\mu$m to ensure there is no larger HA particle for proper measurement within the operational size limit of the DLS instrument. Each sample was measured in triplicate, and average size and $\zeta$-potential were reported with standard deviation (SD).

Attenuated total reflectance-Fourier transform infrared (ATR-FTIR) study was carried out to investigate the chemical compositions of the HA particles. A PerkinElmer Spectrum 100 FTIR spectrometer equipped with a diamond crystal ATR accessory was used for this purpose. The particles were freeze-dried, and the powder was used for spectra recording in the wavenumber region of 4000−1000 cm$^{-1}$ with a resolution of 4 cm$^{-1}$.

The thermal stability of the particles was determined by thermogravimetric analysis (TGA) using Q500 Thermogravimetric Analyzers. The thermogravimetry measurements were carried out under continuous N$_2$ flow (200 mL/min). The heating rate was 10 °C/min to reach up to 950 °C.

SEM (FEI Quanta 200) study was also performed to monitor the morphology of different particles. Samples were separately embedded on the SEM holder covered by a double-sided carbon adhesive tape. The particles were then dried at room temperature overnight and then sputtered by Pt in a high vacuum evaporator before imaging.

**4.4. Cell Lines and Culturing Condition.** Peripheral blood mononuclear cells (PBMC), KG-1 macrophage cells, and J774A.1 macrophages were used for different studies of the present work. Iscove's modified Dulbecco's medium and Dulbecco's modified Eagle's medium (DMEM) were used for the KG-1 and J774A.1, respectively. The media used in this study were supplemented with 10% (v/v) fetal FBS, 1% L-glutamine, penicillin (100 IU/mL), 1% nonessential amino acids, and streptomycin (100 mg/mL) (all from HyClone). The cells were obtained from American Type Culture Collection and cultured in 75 cm$^2$ culture flasks (Corning Inc. Life Sciences). Cells were cultured in a standard gas incubator with the conditions of 95% humidity, 5% CO$_2$, and 37 °C. Confluency of 80% was considered for the subculturing of the cells. Phosphate buffer solution−ethylenediaminetetraacetic acid (PBS−EDTA) solution was used for cell detachment prior to passaging, as well as prior to each experiment.

**4.5. Cellular Cytotoxicity.** The ATP activity of the cells was investigated for cytocompatibility assessment because it is representative of mitochondrial function. For this purpose, 100 $\mu$L of the cell suspension (2 × 10$^5$ cells/mL) was seeded in 96-well plates and left in an incubator at 37 °C overnight. Next, the cell media were removed and 100 $\mu$L of the HA particles with the concentrations of 25, 50, 100, 200, 400, and 600 $\mu$g/mL were added into the wells containing cells. After 24 and 48 h of incubating cells with the particles, 100 $\mu$L of the reagent assay (CellTiter-Glo Luminescent Cell Viability Assay, Promega) was added to each well. The 96-well plates were shaken for 2 min at 450 rpm and left at room temperature for 15 min before measuring the luminescence of the wells. Hanks' balanced salt solution (HBSS) buffer solution was used as the negative control and treated similarly as described above and

considered as 100% viability. The results presented are the average of at least three independent measurements.

**4.6. Hemocompatibility Assay.** Heparinized fresh human blood samples were used for the isolation of red blood cells (RBCs). First, 5 mL of blood was mixed with 10 mL of D-PBS and centrifuged at 2500 rpm for 6 min. This step was repeated five times, and the final RBC pellet was used to prepare 5% hematocrit suspension by mixing 1 mL of the packed RBC with 19 mL of D-PBS. The hemolytic effect of the HA particles was investigated by adding 200 $\mu$L of the 5% hematocrit to 800 $\mu$L of the different HA particle suspensions in D-PBS to reach the final concentrations of 100, 200, and 400 $\mu$g/mL. Each of the samples was vortexed for 5 s and subsequently incubated at room temperature for 1, 6, and 24 h. In each time point, the samples were gently vortexed for 5 s and centrifuged at 6000 rpm for 3 min. A 100 $\mu$L amount of the supernatant was withdrawn and added to 96-well plates (Corning Inc. Life Sciences) for the quantification of the lysed hemoglobin at 577 nm. D-PBS and Milli-Q water were used as negative and positive controls, respectively. The results represent the average of, at least, three independent experiments.

**4.7. Arg-1 Activity and Cytokine Measurement.** To study the impact of polymer MW on the polarization of the macrophages, pure particles were exposed to J774A.1 macrophages in the presence or absence of HA particles in different conditions, including (1) in the resting state of macrophages, that is, adding HA particles in the absence of activating agents; (2) with 100 ng/mL of $\gamma$-irradiated lipopolysaccharide (LPS) derived from *Escherichia coli* (Sigma-Aldrich); and (3) with 10 ng/mL interferon-$\gamma$ (IFN-$\gamma$) and 100 ng/mL $\gamma$-irradiated LPS. For all in vitro studies, J774A.1 macrophages were plated at a density of 2.8 × 10$^5$ cells/mL in a 12-well plate (1.2 mL/well) and allowed to adhere overnight before use. HA particles were used at the concentration of 100 $\mu$g/mL for these studies.

Flow cytometry experiment was performed to quantitatively assess the expression of Arg-1 in the cells as an indicator of M2 polarization in macrophages. For this experiment, resting macrophages were treated as described above for 24 h. The well plates were then washed with HBSS−(4-(2-hydroxyethyl)-1-piperazineethanesulfonic acid) (HEPES) (pH 7.4), and cells were harvested using PBS−EDTA solution. Thereafter, detached cells were diluted with 5 mL of HBSS−(4-(2-hydroxyethyl)-1-piperazineethanesulfonic acid) (HEPES) buffer (pH 7.4) and transferred into 15 mL Falcon tubes to separate cells through centrifugation at 1200 rpm for 4 min. Samples were then dispersed in 0.5 mL of 4% paraformaldehyde at room temperature for 10 min under intermittent agitation to maintain a single cell suspension during the fixation process. Cells were centrifuged and washed two times with PBS (pH 7.4) before resuspending in 200 $\mu$L of permeabilization buffer. Next, 10 $\mu$L of fluorescein conjugated Arg-1 antibody (R&D Systems) was added and cells incubated for 30 min at room temperature in the dark. The cells were washed once with permeabilization buffer and transferred into FACS tubes after resuspending in 500 $\mu$L of PBS (pH 7.4) for flow cytometric analysis with a laser excitation wavelength of 488 nm.

TNF-$\alpha$ and IL-10 secreted by macrophages under different treatments were determined by the measurement of the proteins in the supernatant of the cell culture using an enzyme-linked immunosorbent assay (ELISA) kit (R&D Systems) according to the manufacturer's instructions. The amount of

IL-4 loaded into the particles was measured using the ELISA method.[10]

**4.8. Cellular Interaction of the HA Particles with J774A.1 Macrophages.** The cellular interaction of the HMW particles of HA polymer with J774A.1 macrophage cells was performed using the Alexa Fluor 488 conjugated particles. EDC−NHS-mediated labeling of the HA particles was carried out through the previous reports of our group for other nanocarriers.[57] Flow cytometry experiment was conducted to determine the percentage of cells associated with the HA particles. In a 6-well plate, a density of $5 \times 10^5$ cells/well was prepared in 3.5 mL of the culturing medium. After overnight preincubation at 37 °C and 5% $CO_2$, the cells were washed once with HBSS−HEPES buffer (pH 7.4) and incubated with 3.5 mL of fluorescently labeled particles (100 $\mu$g/mL) for 15, 30, 60, 90, and 120 min. Washing was then performed by HBSS−HEPES (pH 7.4) to remove free particles. The cells were detached by 300 $\mu$L of PBS−EDTA and centrifuged within 5 mL of HBSS−HEPES buffer (pH 7.4) at 1200 rpm for 4 min. The cells were resuspended in 700 $\mu$L of the HBSS−HEPES (pH 7.4) and kept in ice for flow cytometry analysis of the samples with a laser excitation wavelength of 488 nm.

**4.9. IL-4 Loading into HA Particles.** To load the IL-4 cytokine within the HMW HA particles, 0.25 mL of HA solution (4 mg/mL) was transferred into a tube containing 500 ng of the IL-4 in 50 $\mu$L. After a gentle vortexing, the mixture was added dropwise into 7.5 mL of isooctane containing 0.2 M of AOT and 0.04 M of 1-HP under vigorous agitation until a clear solution was obtained. Next, 4 $\mu$L of DVS cross-linker was added under vortexing, and the reaction was allowed to complete for 1 h under stirring at room temperature. The procedure was continued similar to the synthesis process without the cytokine. Loaded amount of IL-4 into HA particles was measured through the collection of the supernatant and its analysis by IL-4 ELISA kits right after particle formation.

**4.10. Analyses of CD44, CD206, and CD163 Expressions on Macrophage.** J774A.1 macrophages were plated in six-well plates with a density of $4 \times 10^5$ cells/well, cultured at 37 °C and 5% $CO_2$ overnight. For the evaluation of CD44 expression, unpolarized J774A.1 macrophage cells were treated with bovine albumin serum (BSA; 3% w/v) for 30 min before 1 h staining with antimouse CD44 antibody at room temperature. After washing thrice with PBS (pH 7.4) and fixation with the paraformaldehyde (4%) for 2 h, the cells were imaged by confocal microscopy and analyzed by flow cytometry for the detection of CD44 surface proteins. Nonstained unpolarized J774A.1 macrophage cells were used as control.

For the determination of CD206 and CD163 expressions, the cells were first polarized to M1 phenotype by incubating with IFN-$\gamma$ (100 ng/mL) and LPS (100 ng/mL) for 16 h. They were then treated with IL-4-loaded HA particles (1.2 mL of 100 $\mu$g/mL) and unloaded particles for 48 h. After washing and fixation in 4% paraformaldehyde, 3% w/v BSA was used for 30 min at room temperature to block nonspecific bindings. The cells were then stained with Alexa Fluor 488-antimouse CD206 and CD163 antibodies for 1 h.

**4.11. In Vitro Polarization Studies.** The effect of the IL-4-loaded HA particles on the induction of macrophage switching from M1 to M2 phenotype was assessed by measuring the change in the expression level of inducible nitric oxide synthase 2 (iNOS2) as M1 marker and Arg-1 as M2 marker in J774A.1 macrophages. After the exposure of the cells ($3 \times 10^5$ cells/well) to LPS (100 ng/mL) and IFN-$\gamma$ (100 ng/mL) in 6-well plates for 16 h, the cells were exposed to the IL-4-encapsulated particles (1.2 mL of 100 $\mu$g/mL) and free particles for 24 h. Next, the cells were divided into two groups: (1) washing with PBS and quantification of the expression of iNOS2 and Arg-1 using qPCR (called 24 h samples in the Results and Discussion section) and (2) harvesting the cells and culturing them in the cell culturing medium for 24 h more before qPCR study (called 24 h samples in the Results and Discussion section). The ratio of Arg-1 to iNOS2 was considered as indicative of M1 to M2 polarization efficiency.

**4.12. Data Analysis.** Data were expressed as mean ± standard deviation (SD). Statistical significance was determined by one-way analysis of variance tests to compare statistical significance at a 5% probability level. A probability ($p$) of less than 0.05 was considered statistically significant.

■ **AUTHOR INFORMATION**

**Corresponding Authors**
*E-mail: m.a.shahbazi@helsinki.fi (M.-A.S.).
*E-mail: helder.santos@helsinki.fi (H.A.S.).

**ORCID**
Bruno Sarmento: 0000-0001-5763-7553
Hélder A. Santos: 0000-0001-7850-6309

**Notes**
The authors declare no competing financial interest.

■ **REFERENCES**

(1) Boechat, A. L.; De Oliveira, C. P.; Tarrago, A. M.; Da Costa, A. G.; Malheiro, A.; Guterres, S. S.; Pohlmann, A. R. Methotrexate-Loaded Lipid-Core Nanocapsules Are Highly Effective in the Control of Inflammation in Synovial Cells and a Chronic Arthritis Model. *Int. J. Nanomed.* **2015**, *10*, 6603−6614.

(2) Kuo, R.; Saito, E.; Miller, S. D.; Shea, L. D. Peptide-Conjugated Nanoparticles Reduce Positive Co-Stimulatory Expression and T Cell Activity to Induce Tolerance. *Mol. Ther.* **2017**, *25*, 1676−1685.

(3) Dolati, S.; Babaloo, Z.; Jadidi-Niaragh, F.; Ayromlou, H.; Sadreddini, S.; Yousefi, M. Multiple Sclerosis: Therapeutic Applications of Advancing Drug Delivery Systems. *Biomed. Pharmacother.* **2017**, *86*, 343−353.

(4) Dolati, S.; Sadreddini, S.; Rostamzadeh, D.; Ahmadi, M.; Jadidi-Niaragh, F.; Yousefi, M. Utilization of Nanoparticle Technology in Rheumatoid Arthritis Treatment. *Biomed. Pharmacother.* **2016**, *80*, 30−41.

(5) Pujol-Autonell, I.; Mansilla, M. J.; Rodriguez-Fernandez, S.; Cano-Sarabia, M.; Navarro-Barriuso, J.; Ampudia, R. M.; Rius, A.; Garcia-Jimeno, S.; Perna-Barrull, D.; Caceres, E. M.; et al. Liposome-Based Immunotherapy against Autoimmune Diseases: Therapeutic Effect on Multiple Sclerosis. *Nanomedicine* **2017**, *12*, 1231−1242.

(6) Shah, M.; Edman, M. C.; Janga, S. R.; Shi, P.; Dhandhukia, J.; Liu, S.; Louie, S. G.; Rodgers, K.; MacKay, J. A.; Hamm-Alvarez, S. F. A Rapamycin-Binding Protein Polymer Nanoparticle Shows Potent Therapeutic Activity in Suppressing Autoimmune Dacryoadenitis in a Mouse Model of Sjögren's Syndrome. *J. Controlled Release* **2013**, *171*, 269−279.

(7) Rostamzadeh, D.; Razavi, S. R.; Esmaeili, S.; Dolati, S.; Ahmahi, M.; Sadreddini, S.; Jadidi-Niaragh, F.; Yousefi, M. Application of Nanoparticle Technology in the Treatment of Systemic Lupus Erythematous. *Biomed. Pharmacother.* **2016**, *83*, 1154−1163.

(8) Serra, P.; Santamaria, P. Nanoparticle-Based Autoimmune Disease Therapy. *Clin. Immunol.* **2015**, *160*, 3−13.

(9) Miao, X.; Leng, X.; Zhang, Q. The Current State of Nanoparticle-Induced Macrophage Polarization and Reprogramming Research. *Int. J. Mol. Sci.* **2017**, *18*, No. 336.

(10) Kwon, D.; Cha, B. G.; Cho, Y.; Min, J.; Park, E.-B.; Kang, S.-J.; Kim, J. Extra-Large Pore Mesoporous Silica Nanoparticles for Directing in Vivo M2 Macrophage Polarization by Delivering IL-4. *Nano Lett.* **2017**, *17*, 2747−2756.

(11) Rios de la Rosa, J. M.; Tirella, A.; Gennari, A.; Stratford, I. J.; Tirelli, N. The CD44-Mediated Uptake of Hyaluronic Acid-Based Carriers in Macrophages. *Adv. Healthcare Mater.* **2017**, *6*, No. 1601012.

(12) Jain, S.; Tran, T. H.; Amiji, M. Macrophage Repolarization with Targeted Alginate Nanoparticles Containing IL-10 Plasmid DNA for the Treatment of Experimental Arthritis. *Biomaterials* **2015**, *61*, 162−177.

(13) Martinez, F. O.; Sica, A.; Mantovani, A.; Locati, M. Macrophage Activation and Polarization. *Front. Biosci.* **2008**, *13*, 453−461.

(14) Hoppstädter, J.; Seif, M.; Dembek, A.; Cavelius, C.; Huwer, H.; Kraegeloh, A.; Kiemer, A. K. M2 Polarization Enhances Silica Nanoparticle Uptake by Macrophages. *Front. Pharmacol.* **2015**, *6*. DOI: 10.3389/fphar.2015.00055.

(15) Genin, M.; Clement, F.; Fattaccioli, A.; Raes, M.; Michiels, C. M1 and M2 Macrophages Derived from THP-1 Cells Differentially Modulate the Response of Cancer Cells to Etoposide. *BMC Cancer* **2015**, *15*, No. 577.

(16) Bolon, B. Cellular and Molecular Mechanisms of Autoimmune Disease. *Toxicol. Pathol.* **2012**, *40*, 216−229.

(17) May, R. D.; Fung, M. Strategies Targeting the IL-4/IL-13 Axes in Disease. *Cytokine* **2015**, *75*, 89−116.

(18) Cha, B. G.; Jeong, J. H.; Kim, J. Extra-Large Pore Mesoporous Silica Nanoparticles Enabling Co-Delivery of High Amounts of Protein Antigen and Toll-like Receptor 9 Agonist for Enhanced Cancer Vaccine Efficacy. *ACS Cent. Sci.* **2018**, *4*, 484−492.

(19) Jiang, D.; Liang, J.; Noble, P. W. Hyaluronan as an Immune Regulator in Human Diseases. *Physiol. Rev.* **2011**, *91*, 221−264.

(20) Kogan, G.; Soltés, L.; Stern, R.; Gemeiner, P. Hyaluronic Acid: A Natural Biopolymer with a Broad Range of Biomedical and Industrial Applications. *Biotechnol. Lett.* **2006**, *29*, 17−25.

(21) Ahrens, T.; Assmann, V.; Fieber, C.; Termeer, C.; Herrlich, P.; Hofmann, M.; Simon, J. C. CD44 Is the Principal Mediator of Hyaluronic-Acid-Induced Melanoma Cell Proliferation. *J. Invest. Dermatol.* **2001**, *116*, 93−101.

(22) Cuff, C. A.; Kothapalli, D.; Azonobi, I.; Chun, S.; Zhang, Y.; Belkin, R.; Yeh, C.; Secreto, A.; Assoian, R. K.; Rader, D. J.; et al. The Adhesion Receptor CD44 Promotes Atherosclerosis by Mediating Inflammatory Cell Recruitment and Vascular Cell Activation. *J. Clin. Invest.* **2001**, *108*, 1031−1040.

(23) Vasi, A. M.; Popa, M. I.; Butnaru, M.; Dodi, G.; Verestiuc, L. Chemical Functionalization of Hyaluronic Acid for Drug Delivery Applications. *Mater. Sci. Eng., C* **2014**, *38*, 177−185.

(24) Dosio, F.; Arpicco, S.; Stella, B.; Fattal, E. Hyaluronic Acid for Anticancer Drug and Nucleic Acid Delivery. *Adv. Drug Delivery Rev.* **2016**, *97*, 204−236.

(25) Mizrahy, S.; Raz, S. R.; Hasgaard, M.; Liu, H.; Soffer-Tsur, N.; Cohen, K.; Dvash, R.; Landsman-Milo, D.; Bremer, M. G. E. G.; Moghimi, S. M.; et al. Hyaluronan-Coated Nanoparticles: The Influence of the Molecular Weight on CD44-Hyaluronan Interactions and on the Immune Response. *J. Controlled Release* **2011**, *156*, 231−238.

(26) Krause, D. S.; Spitzer, T. R.; Stowell, C. P. The Concentration of CD44 Is Increased in Hematopoietic Stem Cell Grafts of Patients with Acute Myeloid Leukemia, Plasma Cell Myeloma, and Non-Hodgkin Lymphoma. *Arch. Pathol. Lab. Med.* **2010**, *134*, 1033−1038.

(27) Rayahin, J. E.; Buhrman, J. S.; Zhang, Y.; Koh, T. J.; Gemeinhart, R. A. High and Low Molecular Weight Hyaluronic Acid Differentially Influence Macrophage Activation. *ACS Biomater. Sci. Eng.* **2015**, *1*, 481−493.

(28) Rayahin, J. E.; Buhrman, J. S.; Zhang, Y.; Koh, T. J.; Gemeinhart, R. A. High and Low Molecular Weight Hyaluronic Acid Differentially Influence Macrophage Activation. *ACS Biomater. Sci. Eng.* **2015**, *1*, 481−493.

(29) Erickson, M.; Stern, R. Chain Gangs: New Aspects of Hyaluronan Metabolism 2012, *2012*, 893947. DOI: 10.1155/2012/893947.

(30) Necas, J.; Bartosikova, L.; Brauner, P.; Kolar, J. Hyaluronic Acid (Hyaluronan): A Review. *Vet. Med.* **2008**, *53*, 397−411.

(31) Toole, B. P. Hyaluronan in Morphogenesis. *Semin. Cell Dev. Biol.* **2001**, *12*, 79−87.

(32) Tran, T.-H.; Rastogi, R.; Shelke, J.; Amiji, M. M. Modulation of Macrophage Functional Polarity towards Anti-Inflammatory Phenotype with Plasmid DNA Delivery in CD44 Targeting Hyaluronic Acid Nanoparticles. *Sci. Rep.* **2015**, *5*, No. 16632.

(33) Highley, C. B.; Prestwich, G. D.; Burdick, J. A. Recent advances in hyaluronic acid hydrogels for biomedical applications. *Curr. Opin. Biotechnol.* **2016**, *40*, 35−40.

(34) Collins, M. N.; Birkinshaw, C. Hyaluronic Acid Based Scaffolds for Tissue Engineering - A Review. *Carbohydr. Polym.* **2013**, *92*, 1262−1279.

(35) Mero, A.; Campisi, M. Hyaluronic Acid Bioconjugates for the Delivery of Bioactive Molecules. *Polymers* **2014**, *6*, 346−369.

(36) McKee, C. M.; Penno, M. B.; Cowman, M.; Burdick, M. D.; Strieter, R. M.; Bao, C.; Noble, P. W. Hyaluronan (HA) Fragments Induce Chemokine Gene Expression in Alveolar Macrophages. The Role of HA Size and CD44. *J. Clin. Invest.* **1996**, *98*, 2403−2413.

(37) Kothapalli, D.; Zhao, L.; Hawthorne, E. A.; Cheng, Y.; Lee, E.; Puré, E.; Assoian, R. K. Hyaluronan and CD44 Antagonize Mitogen-Dependent Cyclin D1 Expression in Mesenchymal Cells. *J. Cell Biol.* **2007**, *176*, 535−544.

(38) Baeva, L. F.; Lyle, D. B.; Rios, M.; Langone, J. J.; Lightfoote, M. M. Different Molecular Weight Hyaluronic Acid Effects on Human Macrophage Interleukin 1β Production. *J. Biomed. Mater. Res., Part A* **2014**, *102*, 305−314.

(39) Kothapalli, D.; Flowers, J.; Xu, T.; Puré, E.; Assoian, R. K. Differential Activation of ERK and Rac Mediates the Proliferative and Anti-Proliferative Effects of Hyaluronan and CD44. *J. Biol. Chem.* **2008**, *283*, 31823−31829.

(40) Puré, E.; Cuff, C. A. A Crucial Role for CD44 in Inflammation. *Trends Mol. Med.* **2001**, *7*, 213−221.

(41) Shahbazi, M. A.; Hamidi, M.; Mäkilä, E. M.; Zhang, H.; Almeida, P. V.; Kaasalainen, M.; Salonen, J. J.; Hirvonen, J. T.; Santos, H. A. The Mechanisms of Surface Chemistry Effects of Mesoporous Silicon Nanoparticles on Immunotoxicity and Biocompatibility. *Biomaterials* **2013**, *34*, 7776−7789.

(42) Shahbazi, M. A.; Almeida, P. V.; Correia, A.; Herranz-Blanco, B.; Shrestha, N.; Mäkilä, E.; Salonen, J.; Hirvonen, J.; Santos, H. A. Intracellular Responsive Dual Delivery by Endosomolytic Polyplexes Carrying DNA Anchored Porous Silicon Nanoparticles. *J. Controlled Release* **2017**, *249*, 111−122.

(43) Reese, T. A.; Liang, H.-E.; Tager, A. M.; Luster, A. D.; Van Rooijen, N.; Voehringer, D.; Locksley, R. M. Chitin Induces Tissue Accumulation of Innate Immune Cells Associated with Allergy. *Nature* **2007**, *447*, 92−96.

(44) Amura, C. R.; Kamei, T.; Ito, N.; Soares, M. J.; Morrison, D. C. Differential Regulation of Lipopolysaccharide (LPS) Activation Pathways in Mouse Macrophages by LPS-Binding Proteins. *J. Immunol.* **1998**, *161*, 2552−2560.

(45) Liu, Y. C.; Zou, X. B.; Chai, Y. F.; Yao, Y. M. Macrophage Polarization in Inflammatory Diseases. *Int. J. Biol. Sci.* **2014**, *10*, 520−529.

(46) Schultze, J. L.; Schmieder, A.; Goerdt, S. Macrophage Activation in Human Diseases. *Semin. Immunol.* **2015**, *27*, 249−256.

(47) Gordon, S.; Martinez, F. O. Alternative Activation of Macrophages: Mechanism and Functions. *Immunity* **2010**, *32*, 593−604.

(48) Mosser, D. M.; Edwards, J. P. Exploring the Full Spectrum of Macrophage Activation. *Nat. Rev. Immunol.* **2008**, *8*, 958−969.

(49) Zhang, Q.; Chen, S.; Zhuo, R. X.; Zhang, X. Z.; Cheng, S. X. Self-Assembled Terplexes for Targeted Gene Delivery with Improved Transfection. *Bioconjug. Chem.* **2010**, *21*, 2086−2092.

(50) Campbell, L.; Saville, C. R.; Murray, P. J.; Cruickshank, S. M.; Hardman, M. J. Local Arginase 1 Activity Is Required for Cutaneous Wound Healing. *J. Invest. Dermatol.* **2013**, *133*, 2461−2470.

(51) Porcheray, F.; Viaud, S.; Rimaniol, A. C.; Léone, C.; Samah, B.; Dereuddre-Bosquet, N.; Dormont, D.; Gras, G. Macrophage Activation Switching: An Asset for the Resolution of Inflammation. *Clin. Exp. Immunol.* **2005**, *142*, 481−489.

(52) Mantovani, A.; Biswas, S. K.; Galdiero, M. R.; Sica, A.; Locati, M. Macrophage Plasticity and Polarization in Tissue Repair and Remodelling. *J. Pathol.* **2013**, *229*, 176−185.

(53) Alvarez, M. M.; Liu, J. C.; Trujillo-de Santiago, G.; Cha, B. H.; Vishwakarma, A.; Ghaemmaghami, A. M.; Khademhosseini, A. Delivery Strategies to Control Inflammatory Response: Modulating M1−M2 Polarization in Tissue Engineering Applications. *J. Controlled Release* **2016**, *240*, 349−363.

(54) Reeves, A. R. D.; Spiller, K. L.; Freytes, D. O.; Vunjak-Novakovic, G.; Kaplan, D. L. Controlled Release of Cytokines Using Silk-Biomaterials for Macrophage Polarization. *Biomaterials* **2015**, *73*, 272−283.

(55) Olefsky, J. M.; Glass, C. K. Macrophages, Inflammation, and Insulin Resistance. *Annu. Rev. Physiol.* **2010**, *72*, 219−246.

(56) Lubberts, E.; Joosten, L. A.; Chabaud, M.; van Den Bersselaar, L.; Oppers, B.; Coenen-De Roo, C. J.; Richards, C. D.; Miossec, P.; van Den Berg, W. B. IL-4 Gene Therapy for Collagen Arthritis Suppresses Synovial IL-17 and Osteoprotegerin Ligand and Prevents Bone Erosion. *J. Clin. Invest.* **2000**, *105*, 1697−1710.

(57) Shahbazi, M. A.; Almeida, P. V.; Correia, A.; Herranz-Blanco, B.; Shrestha, N.; Mäkilä, E.; Salonen, J.; Hirvonen, J.; Santos, H. A. Intracellular Responsive Dual Delivery by Endosomolytic Polyplexes Carrying DNA Anchored Porous Silicon Nanoparticles. *J. Controlled Release* **2017**, *249*, 111−122.